Supporting information

Sustained-Release Method for the Directed Synthesis of ZIF-Derived Ultra-Fine Co-N-C ORR Catalysts with Embedded Co Quantum Dots

Han Ye,[ab] Liangjun Li,*[a] Dandan Liu,[a] Qiuju Fu,[ab] Fuzhao Zhang, [ab] Pengcheng Dai,[a] Xin Gu,[a] and Xuebo Zhao,*[ab]

a. College of New Energy, China University of Petroleum (East China), Qingdao, 266580, P. R. China.

b. State Key Laboratory of Heavy Oil Processing, College of Chemical Engineering, China University of Petroleum (East China), Qingdao, 266580, P. R. China.

Corresponding authors: lilj@upc.edu.cn (L. J. Li) and zhaoxuebo@upc.edu.cn (X. B. Zhao)

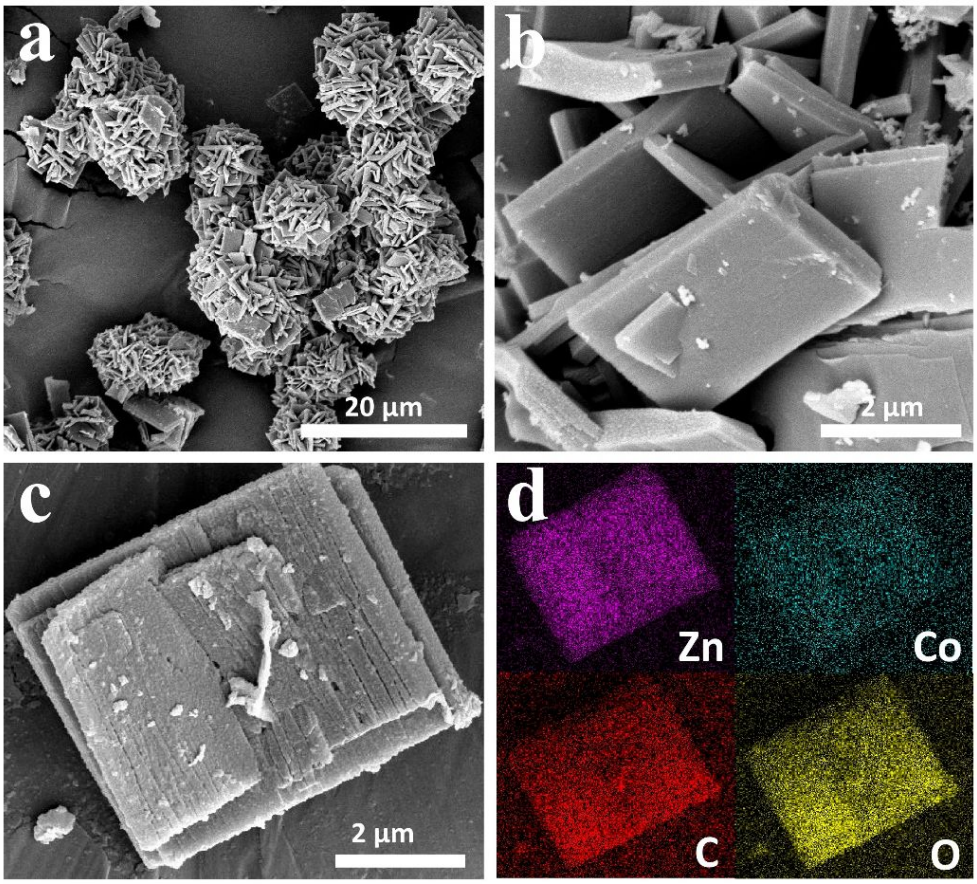

Figure S1. (a-b) SEM images of BZA; (c) SEM image of Co-BZA; (d) elemental mapping of Co-BZA.

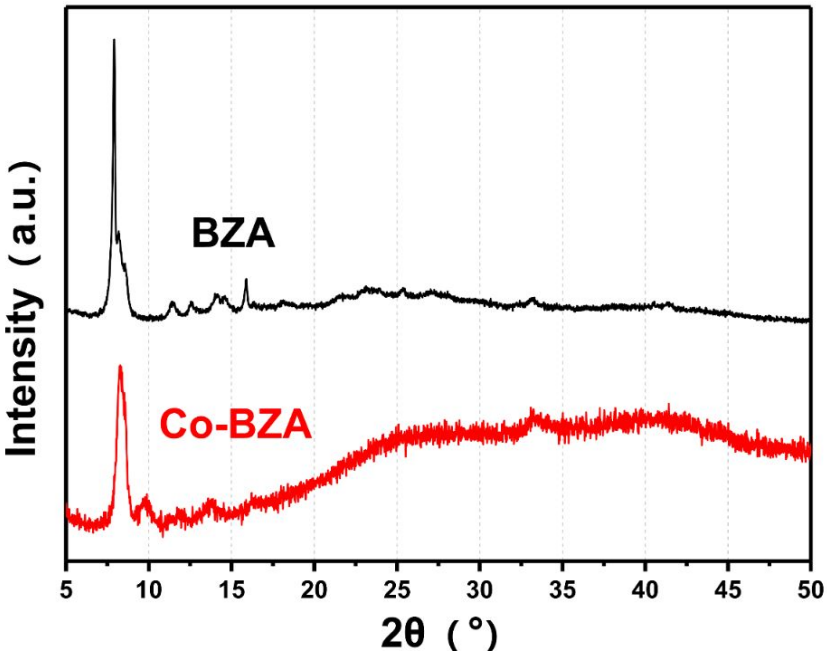

Figure S2. Powder XRD patterns of BZA and Co-BZA

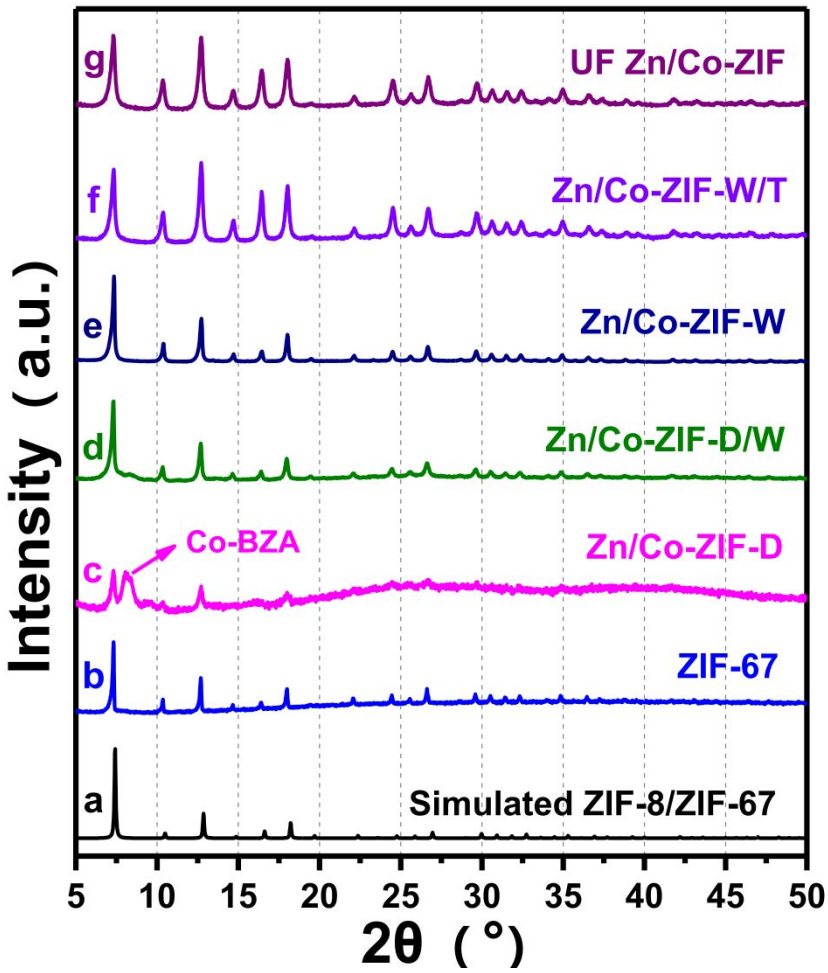

Figure S3. Powder XRD patterns of the ZIF-67 and the as-prepared Zn/Co-ZIFs synthesized in different solvents.

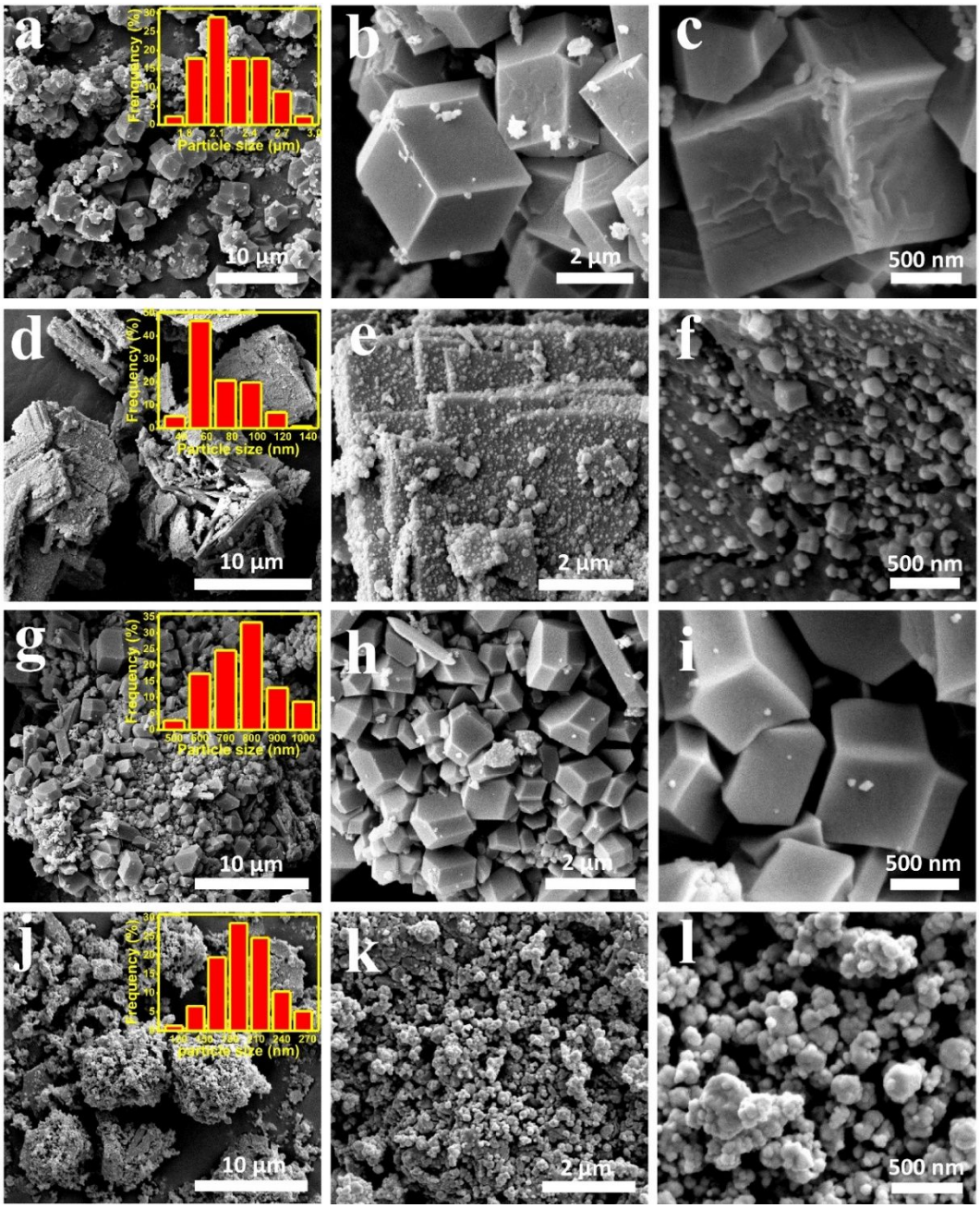

Figure S4. (a-c) SEM images of Zn/Co-ZIF-W (average particle size of 2.3 μm); (d-f) SEM images of Zn/Co-ZIF-D (average particle size of 60 nm); (g-i) SEM images of Zn/Co-ZIF-D/W (average particle size of 750 nm); (j-l) SEM images of Zn/Co-ZIF-W/T (average particle size of 200 nm). (insert is the corresponding particle size distribution)

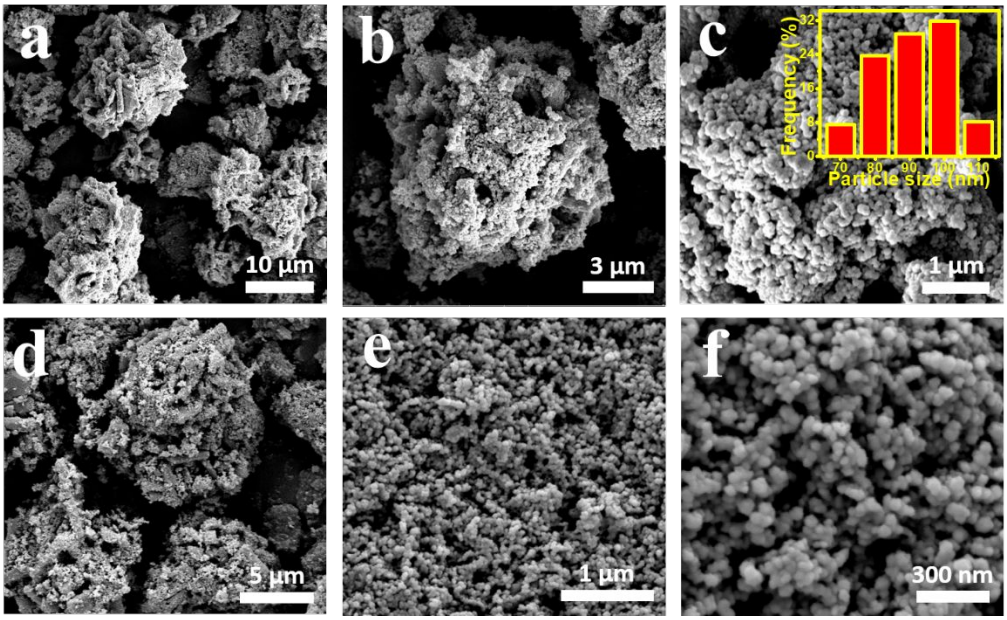

Figure S5. (a-c) SEM images of UF Zn/Co-ZIF; (d-f) SEM images of UF Co-N-C catalyst (insert is the corresponding particle size distribution).

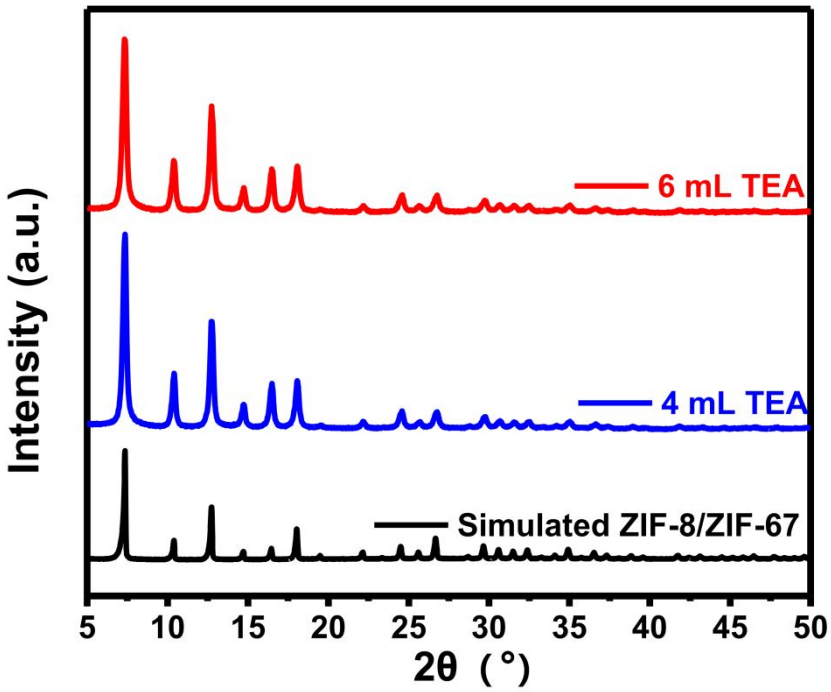

Figure S6. Powder XRD patterns of the as-prepared Zn/Co-ZIFs synthesized in different mixed solvents. Condition A: Zn/Co-ZIF-D/W/T synthesized in a mixed solvent of 1mL DMF, 12mL water and 4mL TEA; condition B: Zn/Co-ZIF-D/W/T synthesized in a mixed solvent of 1mL DMF, 10mL water and 6mL TEA.

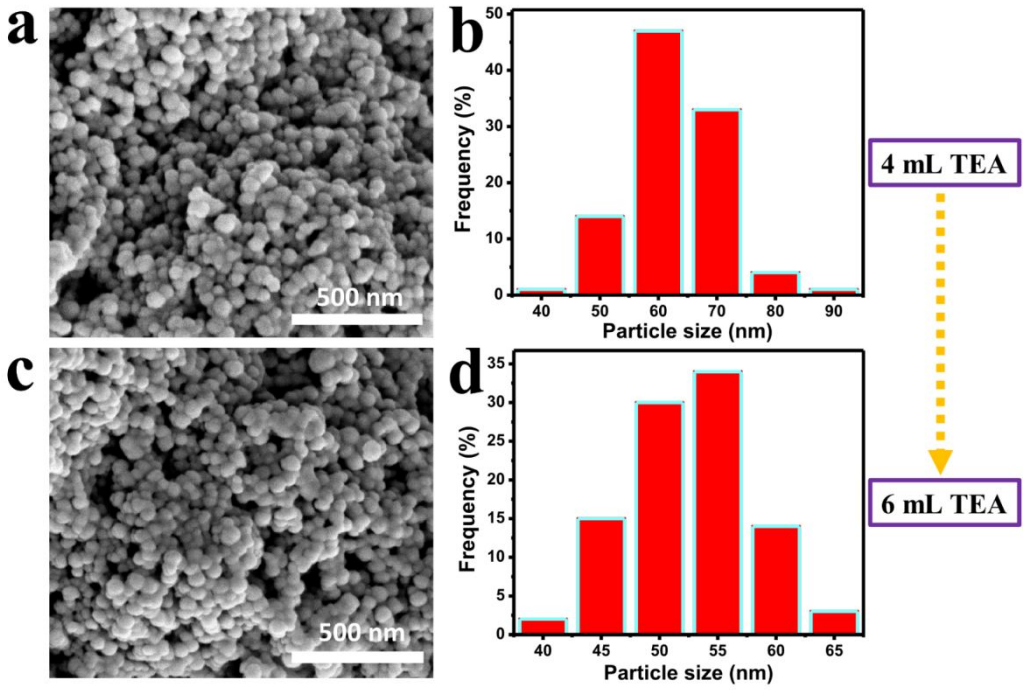

Figure S7. (a-b) SEM image and particle size distribution image of Zn/Co-ZIF-D/W/T synthesized in a mixed solvent of 1mL DMF, 12mL water and 4mL TEA; (c-d) SEM image and particle size distribution image of Zn/Co-ZIF-D/W/T synthesized in a mixed solvent of 1mL DMF, 10mL water and 6mL TEA.

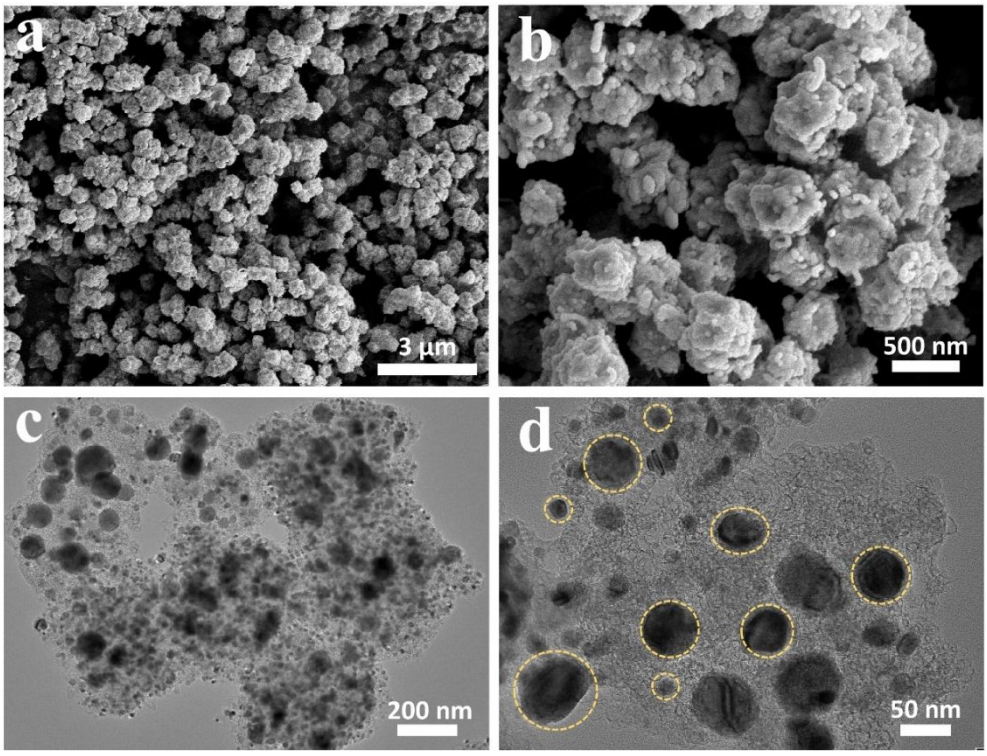

Figure S8. (a, b) SEM images and (c, d) TEM images of ZIF-67-C.

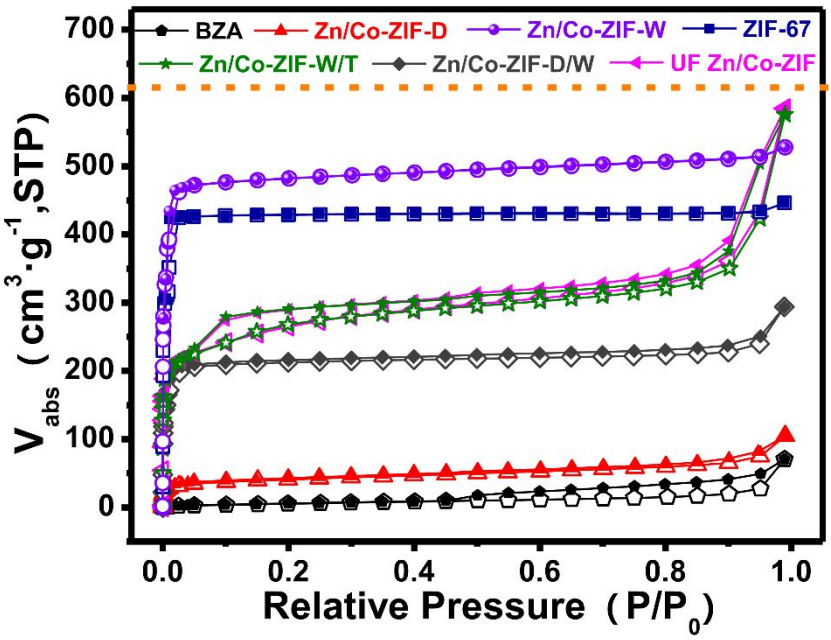

Figure S9. N_2 adsorption-desorption isotherms of BZA, ZIF-67 and the as-prepared Zn/Co-ZIF synthesized in different solvents.

Table S1. Surface area and pore structure parameters of BZA, precursors and derived catalysts calculated from N_2-adsorption/desorption isotherms

Sample	Surface area (m^2 g^{-1})	Micro surface area (m^2 g^{-1})	Total pore volume (cm^3 g^{-1})	Micropore volume (cm^3 g^{-1})
BZA	23	0	0.071	0
Zn/Co-ZIF-D	150	78	0.116	0.032
Zn/Co-ZIF-D/W	879	832	0.344	0.308
Zn/Co-ZIF-W/T	952	728	0.699	0.316
UF Zn/Co-ZIF	958	690	0.711	0.299
ZIF-67	1826	1806	0.601	0.6
Zn/Co-ZIF-W	2102	1999	0.703	0.701
ZIF-67-C	244	114	0.223	0.059
UF Co-N-C	765	539	0.624	0.222

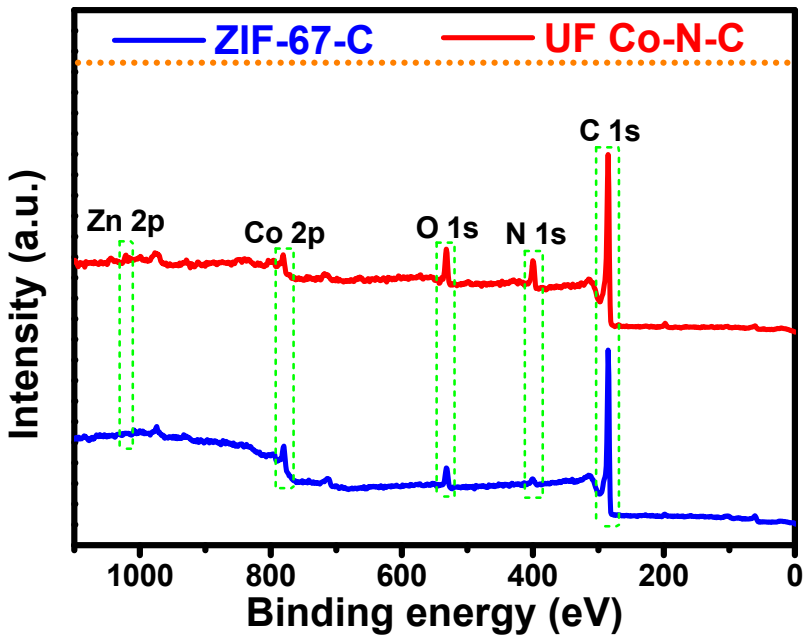

Figure S10. Full XPS spectra of ZIF-67-C and UF Co-N-C

Table S2. Elemental analysis results of ZIF-67-C and UF Co-N-C based on the fitting data of XPS

Sample	Element atomic content (%)				
	Co	**Zn**	**N**	**O**	**C**
ZIF-67-C	14.76	0	3.27	11.77	70.20
UF Co-N-C	6.22	0.84	11.29	15.13	66.52

Table S3. Elemental analysis results of ZIF-67-C and UF Co-N-C based on ICP data

Sample	Element weight content (%)	
	Co	**Zn**
ZIF-67-C	43.32	0
UF Co-N-C	2.83	0.04

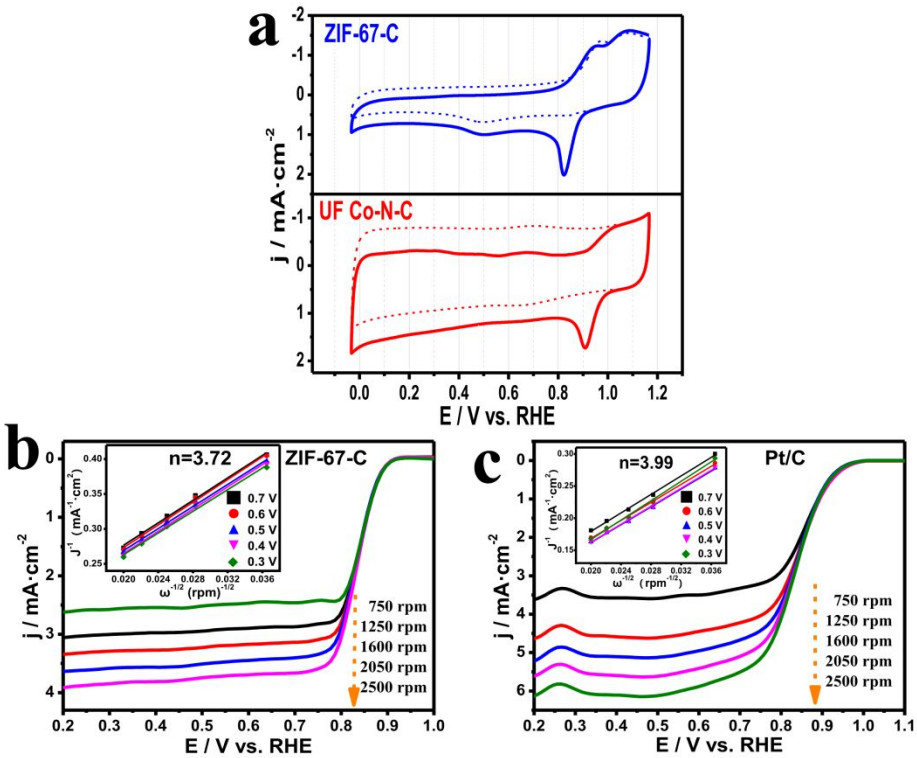

Figure S11. The electrocatalytic ORR performance was tested in 0.1 M KOH. (a) CV curves of ZIF-67-C and UF Co-N-C in N_2- (dotted line) and O_2- (solid line) saturated electrolyte with a scan rate of 10 mV s^{-1}; (b-c) LSV curves of ZIF-67-C and Pt/C at various rotating speed and the corresponding electron transfer number (n) calculated by K-L equation.

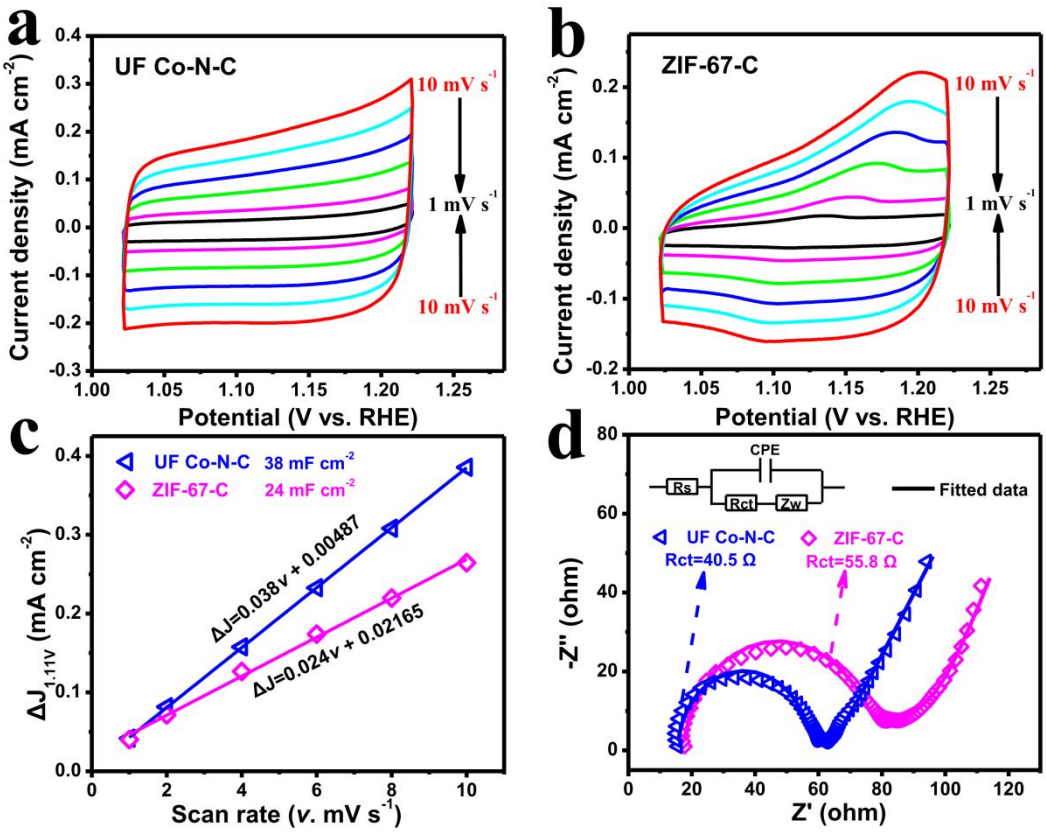

Figure S12. The electrocatalytic ORR performance was tested in 0.1 M KOH. (a-b) CV curves for different samples with scan rate ranging from 1 to 10 mV s^{-1} in N_2-saturated electrolyte; (c) The capacitive currents at 1.11 V as a function of scan rate for UF Co-N-C and ZIF-67-C; (d) Electrochemical Impedance Spectroscopy (EIS) spectra of UF Co-N-C and ZIF-67-C measured at 0.3 V (vs. RHE).

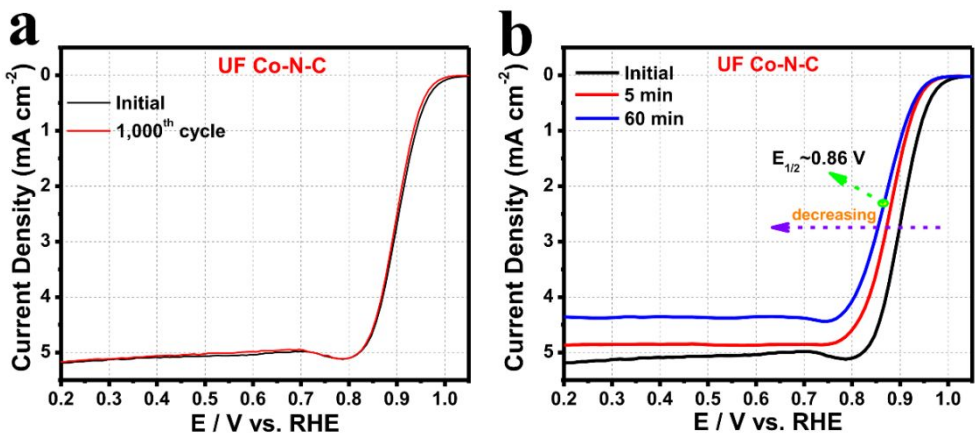

Figure S13. The electrocatalytic ORR performance was tested in 0.1 M KOH at 1600 rpm. (a) ORR polarization plots of the UF Co-N-C before and after 1000 cycles; (b) Time-dependent steady-state ORR polarization curves of 0.01 M KSCN poisoned UF Co-N-C (CV tests measured between 0.6 V and 1 V (vs. RHE) in poison process).

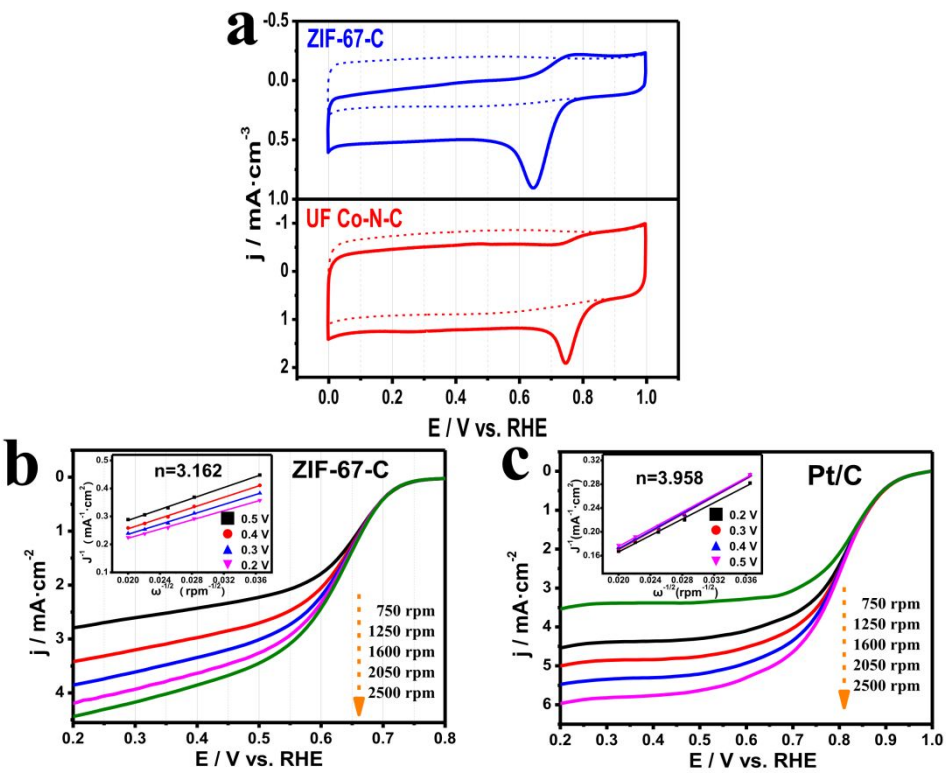

Figure S14. The electrocatalytic ORR performance was tested in 0.5 M H_2SO_4. (a) CV curves of ZIF-67-C and UF Co-N-C in N_2- (dotted line) and O_2- (solid line) saturated electrolyte with a scan rate of 10 mV s^{-1}; (b-c) LSV curves of ZIF-67-C and Pt/C at various rotating speed and the corresponding electron transfer number (n) calculated by K-L equation.

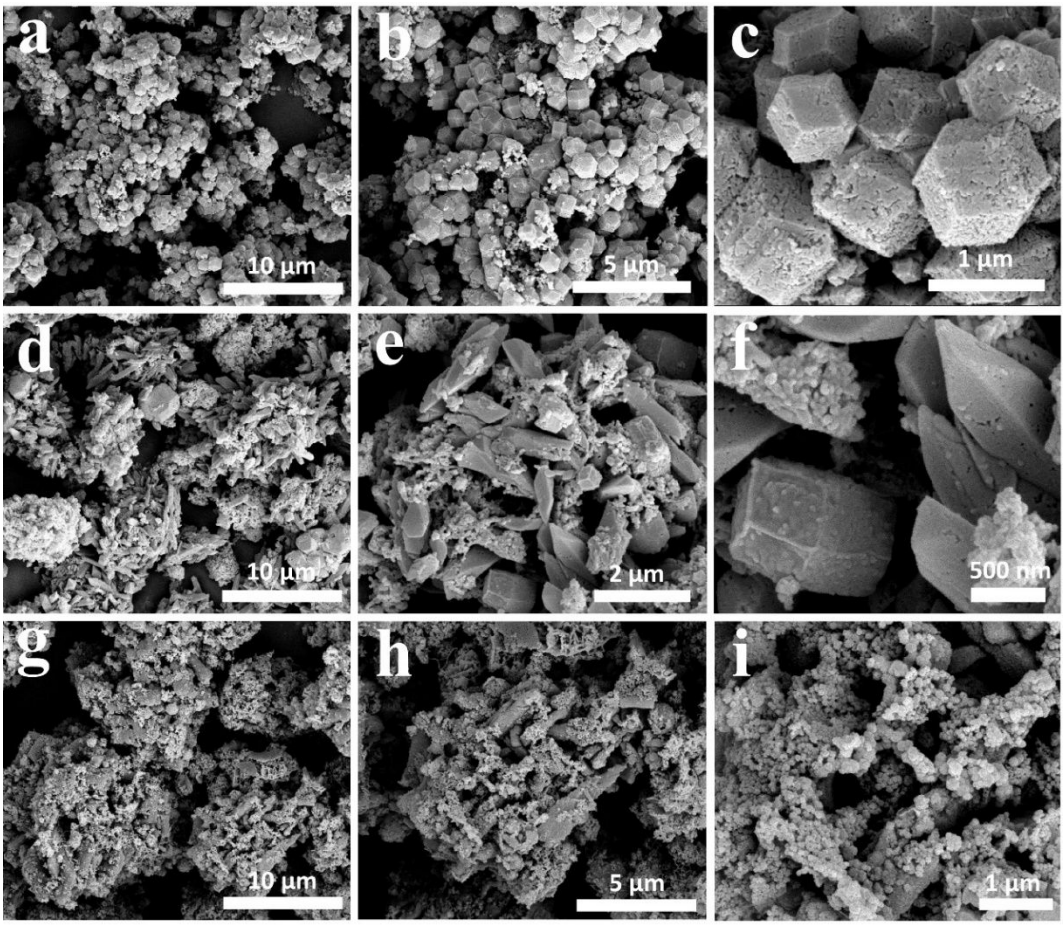

Figure S15. (a-c) SEM images of Co-N-C-W; (d-f) SEM images of Co-N-C-D/W; (g-i) SEM images of Co-N-C-W/T.

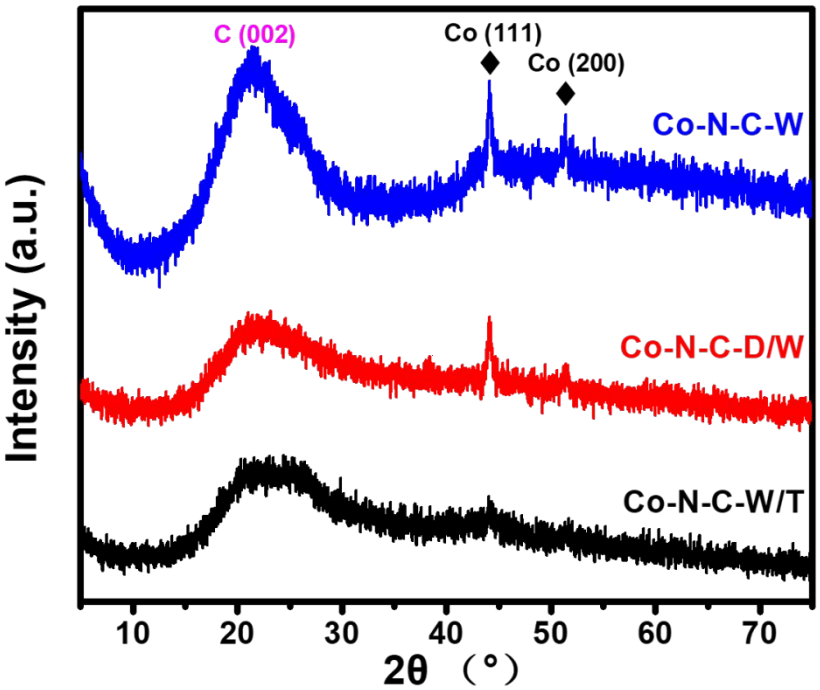

Figure S16. Powder XRD patterns of Co-N-C-W, Co-N-C-D/W and Co-N-C-W/T.

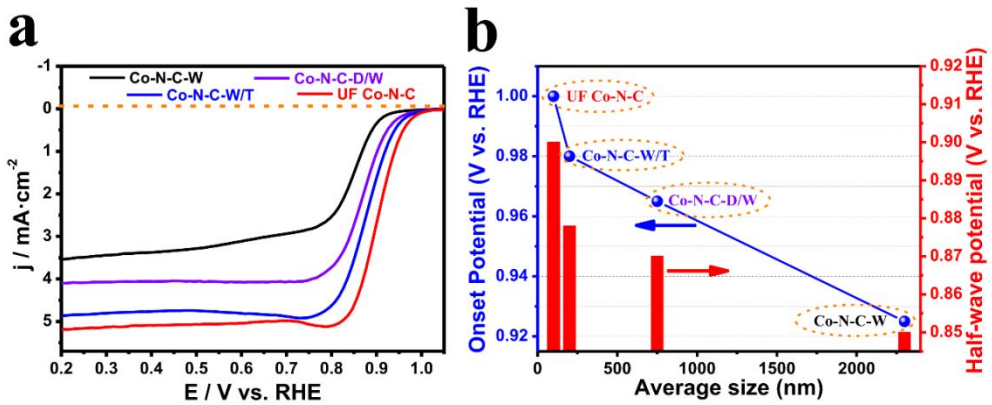

Figure S17. The electrocatalytic ORR performance tests in 0.1 M KOH. (a) LSV curves of Co-N-C-W, Co-N-C-D/W, Co-N-C-W/T and UF Co-N-C. (b) The relationship between average particle size and catalytic performance (onset potential and half-wave potential) based on SEM and LSV results. (The average size is calculated from the precursor before pyrolysis)

Table S4. Comparison of performance for UF Co-N-C and other electrocatalysts recently reported in 0.1M KOH

Materials	**Loading (mg cm^{-2})**	**Onset potential (V vs. RHE)**	**Half-wave potential (V vs. RHE)**	**Limited current (mA cm^{-2})**	**Ref.**
UF Co-N-C	0.48	1.0	0.90	5.2	This work
Fe/Co-N/S-C	0.34	0.95	0.832	5.67	1
Co-Nx/C NRA	0.51	0.99	0.877	5.3	2
Co,N-PCL	0.2	0.94	0.846	5.22	3
Co SAs/N-C (900)	0.408	1.0	0.881	5.6	4
UNT Co SAS/N-C	0.4	0.97	0.89	5.1	5
$Co_{0.6}$-N/C-800	0.254	0.916	0.825	5.2	6
NC@Co-NGC DSNC	0.4	0.92	0.82	4.5	7
Co/N-MC-2-750	0.85	1.0	0.84	5.8	8
Co-N-C-0.8 NPHs	0.283	0.982	0.871	5.35	9
P-Fe-N-CNFs	-	0.94	0.82	5.05	10
FeTMPPCl	0.6	0.936	0.87	5.4	11
Co-N-GA	0.61	0.99	0.85	3.6	12
N-HsGDY-900℃	0.4	1.02	0.85	6.5	14
MCB-3	-	0.937	0.858	6.18	16
NFLGDY-900c	0.6	1.0	0.87	5.3	17

Table S5. Comparison of performance for UF Co-N-C and other electrocatalysts recently reported in acid solution.

Materials	**Loading (mg cm^{-2})**	**Onset potential (V vs. RHE)**	**$E_{1/2}$ (V vs. RHE)**	**Limited current (mA cm^{-2})**	**Electrolyte**	**Ref.**
UF Co-N-C	0.48	0.87	0.75	5	0.5M H_2SO_4	This work
Co-N-C-0.8 NPHs	0.6	0.85	0.761	5.1	0.1M $HClO_4$	9
P-Fe-N-CNFs	0.6	0.85	0.74	5.5	0.1M $HClO_4$	10
FeTMPPCl	0.6	0.824	0.75	4.43	0.1M $HClO_4$	11
Co-N-GA	0.61	0.88	0.73	5.8	0.5M H_2SO_4	12
HC-5Co95Zn	0.5	0.88	0.78	5.7	0.1M $HClO_4$	13
N-HsGDY-900 °C	0.4	0.86	0.64	4.7	0.1M $HClO_4$	14
Fe_3/C-700	0.6	0.90	0.73	4.2	0.1M $HClO_4$	15
NFLGDY-900c	0.6	0.83	≈0.7	4.8	0.1M $HClO_4$	17
$Co_{0.50}Mo_{0.50}N_y$/NCNCs	0.098	0.808	0.62	4	0.5M H_2SO_4	18
ISAS-Co/HNCS	0.5	0.83	0.773	5.61	0.5M H_2SO_4	19

Table S6. The detailed reaction conditions for all of the prepared sample

Sample	Solvent conditions (total volume of 17 mL)			Reaction procedures
	Water (mL)	DMF (mL)	TEA (mL)	
Zn/Co-ZIF-W	17	0	0	
Zn/Co-ZIF-D	0	17	0	
Zn/Co-ZIF-D/W	4	13	0	100 ℃ for 12 h
Zn/Co-ZIF-W/T	15	0	2	
UF Zn/Co-ZIF	14	1	2	

References

1. Li, C.; Liu, H.; Yu, Z., Novel and Multifunctional Inorganic Mixing Salt-Templated 2D Ultrathin Fe/Co-N/S-Carbon Nanosheets as Effectively Bifunctional Electrocatalysts for Zn-Air Batteries. *Appl. Catal. B: Environ.* **2019**, 241, 95-103.

2. Amiinu, I. S.; Liu, X.; Pu, Z.; Li, W.; Li, Q.; Zhang, J.; Tang, H.; Zhang, H.; Mu, S. J. A. F. M., From 3D ZIF Nanocrystals to Co–N_x/C Nanorod Array Electrocatalysts for ORR, OER, and Zn–Air Batteries. *Adv. Funct. Mater.* **2018**, 28 (5), 1704638.

3. Park, H.; Oh, S.; Lee, S.; Choi, S.; Oh, M., Cobalt- and Nitrogen-Codoped Porous Carbon Catalyst Made from Core–Shell Type Hybrid Metal–Organic Framework (ZIF-L@ZIF-67) and Its Efficient Oxygen Reduction Reaction (ORR) Activity. *Appl. Catal. B: Environ.* **2019**, 246, 322-329.

4. Yin, P.; Yao, T.; Wu, Y.; Zheng, L.; Lin, Y.; Liu, W.; Ju, H.; Zhu, J.; Hong, X.; Deng, Z. J. A. C., Single Cobalt Atoms with Precise N-Coordination as Superior Oxygen Reduction Reaction Catalysts. *Angew. Chem. Int. Ed.* **2016**, 128 (36), 10958-10963.

5. Sun, X.; Sun, S.; Gu, S.; Liang, Z.; Zhang, J.; Yang, Y.; Deng, Z.; Wei, P.; Peng, J.; Xu, Y.; Fang, C.; Li, Q.; Han, J.; Jiang, Z.; Huang, Y., High-Performance Single Atom Bifunctional Oxygen Catalysts Derived from ZIF-67 Superstructures. *Nano Energy* **2019**, 61, 245-250.

6. Li, J.; Xia, W.; Tang, J.; Tan, H.; Wang, J.; Kaneti, Y. V.; Bando, Y.; Wang, T.; He, J.; Yamauchi, Y., MOF Nanoleaves as New Sacrificial Templates for the Fabrication of Nanoporous Co–N_x/C Electrocatalysts for Oxygen Reduction. *Nanoscale Horiz.* **2019**, 4 (4), 1006-1013.

7. Liu, S.; Wang, Z.; Zhou, S.; Yu, F.; Yu, M.; Chiang, C. Y.; Zhou, W.; Zhao, J.; Qiu, J. J. A. M., Metal–Organic - Framework - Derived Hybrid Carbon Nanocages as a Bifunctional Electrocatalyst for Oxygen Reduction and Evolution. *Adv. Mater.* **2017**, 29 (31), 1700874.

8. Liu, L.; Ci, S.; Bi, L.; Jia, J.; Wen, Z., Three-Dimensional Nanoarchitectures of Co Nanoparticles Inlayed on N-doped Macroporous Carbon as Bifunctional Electrocatalysts for Glucose Fuel Cells. *J. Mater. Chem. A* **2017**, 5 (28), 14763-14774.

9. You, B.; Jiang, N.; Sheng, M.; Drisdell, W. S.; Yano, J.; Sun, Y., Bimetal-Organic Framework Self-Adjusted Synthesis of Support-Free Nonprecious Electrocatalysts for Efficient Oxygen Reduction. *ACS Catal.* **2015**, 5 (12), 7068-7076.

10. Hu, B.-C.; Wu, Z.-Y.; Chu, S.-Q.; Zhu, H.-W.; Liang, H.-W.; Zhang, J.; Yu, S.-H., SiO_2-Protected Shell Mediated Templating Synthesis of Fe–N-Doped Carbon Nanofibers and Their Enhanced Oxygen Reduction Reaction Performance. *Energy Environ. Sci.* **2018**, 11 (8), 2208-2215.

11. Li, J.; Song, Y.; Zhang, G.; Liu, H.; Wang, Y.; Sun, S.; Guo, X. J. A. F. M., Pyrolysis of Self-Assembled Iron Porphyrin on Carbon Black as Core/Shell Structured Electrocatalysts for Highly Efficient Oxygen Reduction in Both Alkaline and Acidic Medium. *Adv. Funct. Mater.* **2017**, 27 (3), 1604356.

12. Fu, X.; Choi, J. Y.; Zamani, P.; Jiang, G.; Hoque, M. A.; Hassan, F. M.; Chen, Z., Co-N Decorated Hierarchically Porous Graphene Aerogel for Efficient Oxygen Reduction Reaction in Acid. *ACS Appl. Mater. Interfaces* **2016**, 8 (10), 6488-6495.

13. Meng, Z.; Cai, S.; Wang, R.; Tang, H.; Song, S.; Tsiakaras, P., Bimetallic-Organic Framework-Derived Hierarchically Porous Co-Zn-N-C as Efficient Catalyst for Acidic Oxygen Reduction Reaction. *Appl. Catal. B: Environ.* **2019**, 244, 120-127.

14. Lv, Q.; Si, W.; He, J.; Sun, L.; Zhang, C.; Wang, N.; Yang, Z.; Li, X.; Wang, X.; Deng, W.; Long, Y.; Huang, C.; Li, Y., Selectively Nitrogen-Doped Carbon Materials as Superior Metal-Free Catalysts for Oxygen Reduction. *Nat. Commun.* **2018**, 9 (1), 1-11.

15. Hu, Y.; Jensen, J. O.; Zhang, W.; Cleemann, L. N.; Xing, W.; Bjerrum, N. J.; Li, Q. F., Hollow Spheres of Iron Carbide Nanoparticles Encased in Graphitic Layers as Oxygen Reduction Catalysts. *Angew. Chem. Int. Ed.* **2014**, 53 (14), 3675-3679.

16. Ouyang, C.; Ni, B.; Sun, Z.; Zhuang, J.; Xiao, H.; Wang, X., Boosting the ORR Performance of Modified Carbon Black via C-O Bonds. *Chem. Sci.* **2019**, 10 (7), 2118-2123.

17. Zhao, Y.; Wan, J.; Yao, H.; Zhang, L.; Lin, K.; Wang, L.; Yang, N.; Liu, D.; Song, L.; Zhu, J.; Gu, L.; Liu, L.; Zhao, H.; Li, Y.; Wang, D., Few-Layer Graphdiyne Doped with *sp*-Hybridized Nitrogen Atoms at Acetylenic Sites for Oxygen Reduction Electrocatalysis. *Nat. Chem.* **2018**, 10 (9), 924-931.

18. Sun, T.; Wu, Q.; Che, R.; Bu, Y.; Jiang, Y.; Li, Y.; Yang, L.; Wang, X.; Hu, Z., Alloyed Co-Mo Nitride as High-Performance Electrocatalyst for Oxygen Reduction in Acidic Medium. *ACS Catal.* **2015**, 5 (3), 1857-1862.

19. Han, Y.; Wang, Y. G.; Chen, W.; Xu, R.; Zheng, L.; Zhang, J.; Luo, J.; Shen, R. A.; Zhu, Y.;

Cheong, W. C.; Chen, C.; Peng, Q.; Wang, D.; Li, Y., Hollow N-Doped Carbon Spheres with Isolated Cobalt Single Atomic Sites: Superior Electrocatalysts for Oxygen Reduction. *J. Am. Chem. Soc.* **2017**, 139 (48), 17269-17272.